



1 ORCIDs:

2 Jianyang Xia (0000-0001-5923-6665)

3

4 **Title:**

5 TraceME (v1.0) - An online Traceability analysis system for Model Evaluation on
6 land carbon dynamics

7 **Authors:**

8 Jian Zhou¹, Jianyang Xia^{1,*}, Ning Wei¹, Yufu Liu^{2,3}, Chenyu Bian¹, Yuqi Bai^{2,3}, Yiqi
9 Luo⁴

10 **Affiliations:**

11 ¹Research Center for Global Change and Ecological Forecasting, School of Ecological
12 and Environmental Sciences, East China Normal University, Shanghai 200241, China

13 ²Ministry of Education Key Laboratory for Earth System Modelling, Department of
14 Earth System Science, Tsinghua University, Beijing, 100084, China

15 ³Joint Center for Global Change Studies (JCGCS), Beijing, 100875, China

16 ⁴Center for ecosystem science and society, Northern Arizona University, Arizona,
17 Flagstaff, USA

18 *Corresponding author: Jianyang Xia (jyxia@des.ecnu.edu.cn)

19



20 Abstract

21 The synchronous increase of model complexity and data volume in Earth system
22 science challenges using observations to evaluate Earth system models (ESMs). The
23 challenge mainly stems from the untraceable of model outputs, the lack of automatic
24 algorithms, and the high computational costs. Here, we built up an online Traceability
25 analysis system for Model Evaluation (TraceME), which is traceable, automatic and
26 shareable. The TraceME (v1.0) can trace the structural uncertainty of simulated carbon
27 (C) storage in the state-of-the-art ESMs into gross primary production (GPP), carbon
28 use efficiency (CUE), baseline residence time and environmental scalars (temperature
29 and precipitation). The cloud-based framework used in TraceME provides the scientific
30 workflows and a shareable platform to achieve the automated analysis and distributed
31 data storage to greatly improve the efficiency of model evaluation. Then, we set up a
32 worker node in TraceME (v1.0) to store the data from Coupled Model Intercomparison
33 Project (CMIP6), and submitted tasks through browser to analyze the uncertainties of
34 CMIP6 models in the TraceME system. Overall, this new tool can greatly facilitate
35 model evaluation to identify sources of model uncertainty and provide some new
36 implications for the next generation of model evaluation.

37



38 1. Introduction

39 Inter-comparisons among Earth system models (ESMs) as well as between ESMs and
40 data are an essential process to understand the performance of models, reduce their
41 uncertainty, and provide a clear roadmap for model development (Todd-Brown et al.,
42 2013; Eyring et al., 2016a; Getz et al., 2018). As both of the complexity of ESMs
43 increases and the data volume expands rapidly in recent years, the ESMs' evaluation
44 faces many new challenges. For example, the traditional methods used in model
45 evaluation, mainly using statistical approaches, generally treat all metrics equally and
46 ignore their indirect effects on model performance (Schwalm et al., 2010; Xia et al.,
47 2013). Eyring *et al.* (2019a) has suggested that it is suboptimal to give each model equal
48 weight in model evaluation because it is not independence among models. Moreover,
49 model structure contributes approximately 80% of the variance in simulating the land
50 carbon (C) cycle (Bonan and Doney, 2018; Bonan et al., 2019). The climate forcings
51 and model parameters also contribute considerable uncertainty to the performance of
52 ESMs (Ahlström et al., 2012; Shi et al., 2018; Luo and Schuur., 2020). These challenges
53 call for new approaches of model evaluation which can systematically trace and
54 quantify the structural sources of the uncertainty of the componentized models. In
55 addition, the dramatically increase of data in observation and simulation pushes
56 ecological research into a data-rich era (Luo et al., 2011), making it difficult for
57 individuals to do research entirely locally to meet the computational requirements. Thus,
58 an automated computation and shareable platform become essential for a rapid and
59 comprehensive model evaluation. In general, the future approach of model evaluation
60 requires many new characteristics, such as traceable, automatic and shareable.

61 A few efforts have been made to develop new analytical tools for evaluating ESMs,
62 such as the International Land Model Benchmarking (ILAMB) System (Hoffman et al.,
63 2016; Collier et al., 2018), the ESMValTool as a community diagnostic tool with
64 performance metrics for evaluating ESMs (Eyring et al., 2016b), and the Land surface
65 Verification Toolkit (LVT) (Kumar et al., 2012). These analytical tools mainly use many



66 statistical methods and multiple observations as benchmarks to evaluate the complex
67 ESMs. For example, the ILAMB system uses a set of statistical methods to construct a
68 scoring system based on observations as benchmarks to reflect the uncertainties among
69 ESMs (Collier et al., 2018). This benchmarking framework can directly demonstrate
70 the ability of models to simulate given ecological variables through its scores.
71 ESMValTool provides a very comprehensive model evaluation system for ESMs using
72 model outputs from the Coupled Model Intercomparison Project (CMIP) (Eyring et al.,
73 2016b). The LVT can fuse more information to evaluate land surface models, such as
74 remote sensing products and land information system (Kumar et al., 2012). These
75 model evaluation tools can effectively assess the differences between models and
76 observations, as well as the uncertainty among ESMs. Currently, these tools have not
77 yet focused on tracing the uncertainties in land models to their sources in model
78 structures, parameters and external forcings.

79 A traceable model evaluation tool is featured by its ability to systematically
80 quantify model uncertainty source. The traceability analysis method developed by Xia
81 *et al.* (2013) and Luo *et al.* (2017) is a systematic and effective approach to diagnose
82 the uncertainties of terrestrial C-cycle models. It decomposes the C dynamics into C
83 storage and C storage capacity, and uses C storage potential to represent the difference
84 between them. Then, those three variables can be further decomposed into a few
85 traceable components to trace the sources of model uncertainty, such as net primary
86 productivity (NPP), C residence time and environmental factors (temperature and
87 precipitation). This framework has been applied to some model evaluation studies
88 (Rafique et al., 2016; Jiang et al., 2017; Rafique et al., 2017). For example, Xia *et al.*
89 (2013) applied this framework to analyze the differences in modeled C processes among
90 biomes and the effect of nitrogen processes. Du *et al.* (2018) explored the effect of three
91 different carbon-nitrogen coupling schemes on C storage capacity and its responses to
92 atmospheric CO₂ enrichment. Zhou *et al.* (2018) applied the traceability analysis to
93 compare the simulated terrestrial C cycle across 25 models in three MIPs (i.e., CMIP,
94 TRENDY, and MsTMIP). Overall, this traceability analysis framework has the



95 advantage of providing a simple way to explain model variations by using a few
96 traceable components (Xia et al., 2013). Developing it as an available tool for model
97 evaluation can effectively trace and quantify the structural sources of uncertainty in
98 models.

99 Traditional model evaluations need to download large volumes of data from
100 multiple data centers to analyze it locally. For example, the individual users have to
101 repeatedly download model outputs of CMIP5 and CMIP6 from the servers of Earth
102 System Grid Federation (ESGF) for different analyses. However, the data volumes of
103 model outputs and data products both have been increased rapidly in the recent years.
104 For example, the size of database has been increased from 36 TB in CMIP3 to 2.5 PB
105 in CMIP5, and the volume of climate data is expected to 350 PB by 2030 (Overpeck et
106 al., 2011). Thus, it is more and more time-consuming for future researchers to download,
107 manage, preprocess and analyze the CMIP data on their local equipment (Xu et al.,
108 2019). To improve the computational efficiency of processing the data from distributed
109 data sources, it needs a new platform for model evaluation especially in the data
110 computing and storage. Bai *et al.* (2012) has shown that using “everything-shared-over-
111 the-web” to replace the common paradigm of “everything-locally-owned-and-operated”
112 is a promising solution to process distributed data. To achieve this goal, we need to
113 develop the model evaluation tools to be automatic and shareable platform. Thus, a
114 cloud-based framework with the scientific workflow is a good choice for model
115 evaluation. Cloud-based system can combine web-based technology to provide user-
116 friendly web interfaces and automatic workflows. Such web-based technology has been
117 used in the field of ecological modelling and model evaluation. For example,
118 Abramowitz. (2012) has introduced an online model evaluation tool, the Protocol for
119 Analysis of Land Surface models (PALS), to automatically evaluate the performance of
120 model. In addition, Huang et al. (2019) has developed a web-based software system
121 (i.e., Ecological Platform for Assimilating Data; EcoPad v1.0) to realize ecological
122 forecasting. The advantage of the web-based cloud technology can help the researchers
123 to focus on scientific problem of ESMs rather than processing the data.

124 The aim of this paper is to present an online traceability analysis system for model
125 evaluation (TraceME v1.0) to evaluate the ESMs based on the traceability analysis. We
126 first describe the technical aspects of the software system, include the traceability



127 method and data used in the tool, and then use part of the CMIP6 data as examples to
128 demonstrate the functionality of the TraceME. Finally, we discuss the implications of
129 TraceME (v1.0) for the next generation model evaluation and its future developments.

130 **2. TraceME (v1.0):**

131 **2.1 Overview of the TraceME**

132 TraceME (v1.0) is an online framework for automatically analyzing and evaluating the
133 performance of models using the traceability analysis method. It builds on a
134 collaborative analysis framework for distributed gridded environmental data (CAFE;
135 Xu et al. 2019), which consists of at least one central server and more than one worker
136 node. The central node is used to manage the descriptive information about each node,
137 and the data and the available analytic scripts are stored on each worker node. Each
138 node (center and work node) consists of web-based User Interface (UI), data index
139 module, task-managing module and data analysis module. This multi-node structure
140 can realize collaborative analysis of distributed data (More details are described in Xu
141 et al., 2019). TraceME inherits CAFE's ability to collaborate on distributed data, but
142 has different core functions and focuses (Fig. 1). It integrates the traceability analysis
143 and focuses on analyzing and tracing the sources of model uncertainty rather than the
144 flexible data preprocessing in CAFE. In addition, TraceME makes several technical
145 updates to accommodate the processing of multivariate data for the systematic analysis
146 of uncertainty of models. When a user selects the data of interest and sends a request
147 through the web browser, the scientific workflow is triggered. The corresponding tasks
148 are assigned by the central node to the worker node containing the corresponding data,
149 and then running the traceability analysis and returning the results to the user interface
150 (Fig. 1). The major components of Web-based UI, data analysis module and data
151 management module are described below.

152 The web-based UI provides a straightforward way for users to interact with the
153 system through a web browser. It can select data of interest, submit tasks, check the
154 status of tasks and present the results of traceability analysis. The registered users can
155 filter the data of interest by institute, model, frequency and other information of the
156 dataset. After submitting the task, the web-based UI sends requests to the connected
157 node and run the data analysis module. The results of traceability analysis will be saved



158 and a relational database is used to store that information. User can retrieve and
159 visualize the results of both figures and NetCDF files according to traceability analysis
160 through the web-based UI.

161 The data analysis module is to realize the traceability analysis, which can
162 systematically analyze the uncertainty of models and output the corresponding analysis
163 results. It consists of an analysis launcher, a command executor and the traceability
164 analytic script. When the real-time monitoring of the analysis launcher picks up the task,
165 it parses the information of task and instantiates it as a Java command executor. The
166 command executor invokes the analytic script written by Python to run the traceability
167 analysis.

168 The data managing module includes data index submodule and task managing
169 submodule. The data index submodule manages the descriptive information about data
170 (data file name, storage path and data attributes) stored on each worker node. Task
171 managing module is used to task submission, task dispatching, and task status/results
172 query services on each node. The data managing module in the central node is used to
173 maintain the global data and task information. User can scan and update data
174 information by the web-based UI supported by data index module. When user sends the
175 task-by-task managing submodule, the task information will be dispatched to a node
176 and maintained in the database on that node. The task managing submodule in the
177 central server provides global task information retrieval.

178 2.2 Traceability analysis framework

179 The core functionality of TraceME is based on traceability analysis framework of C
180 storage (X) at steady state that developed by Xia *et al.* (2013). This framework is
181 extended to transient dynamic by decomposing the C storage dynamics into a three-
182 dimensional parameter space (Luo et al., 2017). The latter can be further partitioned
183 into traceable components to track the sources of model uncertainty. In the framework
184 of Traceability analysis, terrestrial C storage is at dynamic disequilibrium, which is
185 collectively influenced by internal C-related processes, environmental forces, and their
186 interactions (Luo and Weng, 2011). Under given environmental conditions, the C
187 storage of an ecosystem can reach the steady state, which can be defined as C storage
188 capacity (X_C). In ESMs, we can obtain the X_C by spinning up the model to the steady



state (Xia et al., 2012). Because the external forces, such as climate, are never at steady state, so the X_C is always deviate from the realistic C storage in natural ecosystems. Such deviation or difference between the transient C storage and X_C was defined as C storage potential (X_P) (Luo et al., 2017). Hence, the transient C storage of an ecosystem can be determined by X_C and X_P . Then, X_C is jointly determined by ecosystem C input (e.g., net primary production, NPP) and ecosystem C residence time; (τ_E). As the net ecosystem C input, NPP is determined by gross primary production (GPP) and C use efficiency (CUE). CUE describes the capacity of an ecosystem to effectively absorb C from the atmosphere (DeLucia et al., 2007; Xia et al., 2017). The τ_E can be further traced to the baseline C residence time (τ'_E) and the environmental scalar (ξ). τ'_E represents the ecosystem C residence time under optimal environmental conditions, which is usually determined by the preset soil properties and vegetation characteristic in the model (Xia et al., 2013). The ξ is influenced by several factors, such as climate, oxygen, and land cover. The climate is the most common limiting factor in ESMs. In this study, we focus on the effect of climate forcing (i.e., temperature and precipitation) on the τ'_E . The detail of Traceability analysis method is described in Xia et al. (2013), Luo et al. (2017) and Zhou et al. (2018).

In the framework of traceability analysis, land C storage is ultimately attributed to its traceable components, which are related to the natural properties expressed by the model (Fig. 2). For example, GPP is the photosynthetic property of vegetation; baseline residence time is related to the soil attributes (Fig. 2). In order to quantify the contributions of these traceable components to the uncertainty of models, we use a hierarchical partitioning method (Chevan and Sutherland, 1991) to decompose the uncertainty of simulated C storage dynamics. This method can be used to calculate the independent effect of each explanatory variable ($x_1, x_2, x_3 \dots x_k$) on a single dependent variable (y). The independent effect of x_1 (I_{x1}) means the contribution of x_1 to the variable y , which is calculated by comparing the fit of all models (2^k possible models) including x_1 to that lacking x_1 by the hierarchical partitioning (Chevan and Sutherland, 1991; Murray and Conner, 2009). In our system, we calculate the variance contribution of the variables using the 'hier.part' package in R. First, the C storage can be decomposed into carbon storage capacity and potential. The relative contribution of X_C and X_P to X are estimated. Second, the carbon storage capacity is decomposed into NPP and residence



time. To apply this method, all variables are their logarithmic form: $\ln(X_C)$, $\ln(\text{NPP})$ and $\ln(\tau_E)$. The contributions of NPP and τ_E to X_C are calculated. Third, NPP is further decomposed into GPP and CUE, and residence time is decomposed into baseline residence time and environmental scalars (temperature and precipitation). Convert them into logarithmic form. The contributions of GPP and CUE to NPP are calculated. The contributions of baseline residence time, temperature and precipitation to residence time are calculated as the same way. Finally, the contributions of these traceable components (GPP, CUE, baseline residence time, temperature and precipitation) can be calculated.

2.3 Data

In this study, the TraceME (v1.0) used CMIP6 model outputs as examples to describe the workflow of this platform. The TraceME can be compatible with any model output that follows the Network Common Data Format (netCDF) Climate and Forecast (CF) Metadata Convention (<http://cfconventions.org/>). The data is stored in the database of each node, and the information of data in each node is aggregated to the central node, where users can access and handle all data stored on all nodes of the whole system. On the other hand, TraceME (v1.0) is a systematic framework for uncertainty analysis on the terrestrial carbon cycle for CMIPs. It requires a multivariable dataset to analyze and trace the sources of uncertainty in simulating ecosystem carbon storage. The time series data of total ecosystem carbon storage are needed, which generally consist of vegetation carbon (leaf, woody and root carbon pools), soil carbon (fast, slow and passive soil carbon pools) and/or litter carbon pools (litter and/or coarse woody debris) in the model outputs. The time series data of NPP, GPP and forcing data (temperature and precipitation) are also used for further model intercomparisons. All data used in this study is from 7 CMIP6 models (the release data before July, 2019) and collected from ESGF (<http://esgf.llnl.gov/>) as shown in Table 1.

3. Applications of TraceME (v1.0)

3.1 Temporal dynamics of land carbon storage in CMIP6 models

TraceME (v1.0) provided an automatic traceability analysis for data of temporal interest, which can be used to evaluate the temporal dynamics of land C storage simulated by



models. We used 7 models that had been submitted results in CMIP6 to analyze the uncertainty of these models in simulating historical land carbon storage from 1850 to 2014. Once we selected the data of interest through the browser and submitted the task, the daemon automatically preprocessed the data and ran the temporal traceability script, and returned the results in the forms of figures and data in netCDF format. Under the traceability analysis system, the temporal dynamics of global annual C storage simulated by different models were first calculated (Fig. 3a). The global annual C storage varied greatly among the 7 models, ranging from 938.76 ± 11.36 to 2206.76 ± 50.14 Pg C (Fig. 3a). Decomposing the C storage into C storage capacity and potential, the C storage potential ranged considerably from about -21.66 ± 54.39 to 58.07 ± 57.62 (Fig. 3a). And the C storage capacity of different models in response to external force was also quite different. For example, the lowest simulated C storage capacity was IPSL-CM6A-LR during 1850 to 2014, which was 944 ± 27.14 Pg C, and the other models were from about 1677.57 ± 57.21 to 2263.43 ± 106.61 Pg C (Fig. 3a). To further analyze the uncertainty of C storage capacity, this framework decomposed it into NPP and residence time. These two variables reflected the net C input capacity (38.48 ± 2.72 to 68.74 ± 5.88 Pg C yr⁻¹) and the C turnover time of ecosystem (23.22 ± 1.75 to 56.23 ± 3.10 years) in the models (Fig. 3b-c and 4a). In details, the lowest simulated NPP was CESM2 and the shortest residence time was IPSL-CM6A-LR, while CanESM5 had the largest NPP and residence time among all models (Fig. 3b-c and 4a).

To further trace the uncertainty sources of NPP simulated by models, TraceME (v1.0) decomposed it into GPP and CUE (Fig. 3d-e and 4b). The differences of GPP and CUE in different models reflected the model's photosynthetic capacity and C transfer efficiency from atmosphere to ecosystem biomass. Based on this process, TraceME could quantify the effects of models simulating photosynthesis and respiration on the uncertainty of NPP. For example, NPP simulated by CanESM5 and EC-Earth3-Veg had larger uncertainty, which were 68.74 ± 5.88 and 48.96 ± 2.78 Pg C yr⁻¹ respectively during 1850 to 2014, whereas their GPP was similar, which were 132.22 ± 8.18 and 127.72 ± 4.38 Pg C yr⁻¹ respectively (Fig. 3b-e and 4b). Therefore, the uncertainty of NPP between the two models mainly came from CUE (0.52 ± 0.01 and 0.38 ± 0.02 , respectively), which was related to autotrophic respiration. In addition, residence time was traced to baseline residence time and environmental scalars in TraceME. Baseline residence time explained the uncertainty of some preset attributes



in the model structure, such as soil C decomposition rate, and the environmental scalar reflected the impact of external forces on the performance of model. For example, IPSL-CM6A-LR had the shortest residence time (23.22 1.75 years) than other models during 1850 to 2014, and compared with external forces, the main reason was it had the shortest baseline residence time (18 years) among all models (Fig. 3c, 3f-i and 4c). Hence, the development of IPSL-CM6A-LR was suggested to pay more attention to some preset attributes of soil. Furthermore, the environmental scalar in TraceME here was the global annual scale. Its uncertainty reflected the variability of interannual variation of temperature and precipitation used in each model over all models rather than the direct difference of external forces among models (Fig. 3f-h and 4c-d).

Overall, after analyzing the uncertainties of all traceable components, TraceME summarized the variance contributions of the components to the uncertainty of land C storage among models. This framework traced the uncertainty of land C storage to several sources, and the hierarchical partitioning method could be used to decompose the variation in it into the traceable components. For example, the variation of land C storage among 7 CMIP6 models was mainly from residence time and NPP, and the C storage potential contributed about 4.5% (Fig. 5). Comparing all traceable components, the variation in C storage simulated by these models was dominated by baseline residence time (Fig. 5).

3.2 Spatial distribution of land carbon storage uncertainties in CMIP6 models

TraceME (v1.0) provided the ability to analyze spatial uncertainty of models. It could trace the sources of the uncertainty of models in simulating C storage at each grid. The region of interest in TraceME (v1.0) could be selected by latitude and longitude. Here, we selected global data of 7 CMIP6 models by setting the spatial range according to longitude and latitude through the browser and submitted this task of spatial traceability analysis. When the task was submitted, TraceME (v1.0) extracted data from the entire system for processing and called for spatial traceability analysis scripts. The mean spatial pattern of the 7 models showed C storage in boreal regions was higher than in other regions (Fig. 6a). However, some models, such as IPSL-CM6A-LR, had no such spatial pattern (Fig. 7), and the high variability of C storage simulated by these models also appeared in the boreal regions, such as Siberia and northern North America (Fig. 6b). To further research the sources of the uncertainty of models in simulating C storage,



TraceME (v1.0) provided the spatial patterns of C storage capacity and C storage potential (Fig. 6c-f and 7).

According to traceability framework, TraceME (v1.0) provided the spatial distributions of NPP and residence time to explain the uncertainty of land C storage capacity among models (Fig. 7). From the results of 7 CMIP7 models, the distribution of the variation in NPP among these models occurred in the lower latitude region, while the variation of residence time was mainly distributed in northern high latitude region (Fig. 8a and 8d). Following the workflow of TraceME (v1.0), the uncertainties of global distributions of NPP and residence time were further decomposed into the spatial variations of their traceable components: GPP, CUE, baseline residence time and environmental scalars (Fig. 8b-c and 8e-f). To better guide model development, it is important for model evaluation to provide the information of the spatial distribution of the dominant factor influencing the simulation of land C storage. TraceME (v1.0) could analyze the variation contributions of all traceable components to land C storage at each grid, and offered the spatial pattern of the dominant factor (Fig 9). For example, the baseline residence time and GPP were the major contributors to the global distribution of the variation of simulated C storage by the 7 models from CMIP6 (Fig. 9). Compared to GPP, baseline residence time dominated the uncertainties of simulated land carbon storage in northern high latitude, eastern Asian and the northern part of South America (Fig. 9).

3.3 Uncertainty analysis of simulated carbon storage from models at different periods

Assessing the performances of model over different periods could provide a more comprehensive understanding of the model's ability to simulate land C storage. For example, the environmental scalars among the 7 CMIP6 models had larger variability at initial state (e.g. from 1850 to 1860) than those at current state (e.g. 2004 to 2014) (Fig. 3f). It was necessary to research in detail the sources of uncertainty that different models simulated at different periods. It was convenient for TraceME (v1.0) to submit multiple tasks and perform them simultaneously. We submitted four tasks for temporal and spatial analysis of the performance of 7 CMIP6 models at two periods (1850 to 1860 and 2004 to 2014 presenting initial and current conditions respectively). From the results, the dominant contributor of initial state of models was baseline residence time



that was similar to that at current period (Fig. 10). The variance contribution of C storage potential to C storage simulated by the models at the two periods had larger difference, which was 5.2% and 19.1% at initial and current periods respectively (Fig. 10). In addition, GPP and residence time were also the major contributors to the global distribution of the uncertainty of simulated land C storage at the two periods (Fig. 10). However, the regions where GPP was the dominant contributor of carbon storage variability at initial period were larger than that at current period, especially in the high northern latitudes (Fig. 10).

4. Discussion

4.1 Facilitating the next generation of model evaluation

The increase of model complexity and the expansion of observation promote the model evaluation into the next generation. In our study, we propose that the next generation of model evaluation needs to some new characteristics, including traceable, automatic and shareable. TraceME (v1.0) is designed to meet these three characteristics, and can provide complementary functions to those existing model-evaluation tools. For example, ESMValTool (v1.0) uses observational data (e.g. observations for Model Intercomparison Projections and re-analyses data, obs4MIPs and ana4MIPs) as diagnostics and performance metrics to measure the uncertainty in ESMs (Eyring et al., 2016b). ILAMB constructs a comprehensive set of observation data (e.g. Fluxnet and MODIS) as benchmarks and a scoring system to evaluate the performance of land models (Collier et al., 2018). As the core function of TraceME, the traceability analysis is helpful for extending current model evaluations to quantify the structural sources of the uncertainty of model (Lovenduski et al., 2016). Rather than simply comparing the differences in simulated C storage among models, this method can trace the uncertainties to the carbon storage potential, GPP, CUE, baseline residence time and environmental factors (temperature and precipitation), and quantify the relative variance contributions of these traceable components (Fig. 4 and 8). For example, the annual C storage simulated by IPSL-CM6A-LR is much lower than other models, and TraceME can track it to C storage capacity (Fig. 3a). After a further systematic analysis on C storage capacity, TraceME tracks the low estimates on the global scale in IPSL-CM6A-LR to C residence time, especially the baseline C residence time (Fig. 3-4). Thus, TraceME can not only show the structure sources of the disagreement on global



380 C storage between ESMs, but also identify the key uncertain component for a specific
381 model to facilitate its development.

382 The cloud-based framework adopted by TraceME (v1.0) provides a web-based
383 scientific workflow and shareable platform for automated computation. Compared with
384 the rapid acquisition of observational data, the slow development of ESMs has become
385 one of the bottlenecks to a deeper understanding of ecosystem. As an important part of
386 model development, model evaluation also needs higher computational efficiency. In
387 the absence of automated computation, model evaluation is usually computationally
388 low-efficient due to the repeated computation for each model output. Therefore,
389 automation is a crucial property for an efficient model evaluation. Most model
390 evaluation tools have implemented automation by encapsulating workflows as offline
391 software packages. For example, both ILAMB and ESMValTool have released their
392 second version packages (Collier et al., 2016; Eyring et al., 2019b). TraceME (v1.0)
393 uses the web-based technology to integrate a user-friendly interface and automated
394 computation in background. Users can complete all steps of data processing including
395 submitting task, processing data and managing results through a web browser with a
396 unique ID and web address. The web-based workflow has the advantages of
397 convenience, timeliness and visualization (LeBauer et al., 2013), avoiding the need for
398 technical training for scientific researchers to run packages.

399 Both modeling outputs and observation data come from multiple data sources. For
400 example, model comparison projects have data sources of CMIP, TRENDY and
401 MISMIP. As shown by Song et al. (2019), more than one thousand global-change
402 experiments have been done in the ecology field to monitor the responses of terrestrial
403 C processes to global change. In order to more fully evaluate the performance of models,
404 researchers need to collect large amounts of data from different data sources. The cloud-
405 based technology is considered to be the most effective means to solve the distributed
406 geospatial big data (Bai and Di, 2012; Li et al., 2016). TraceME (v1.0) uses the cloud-
407 based framework that consists of a center node and multiple worker nodes set at
408 different data sources, and the user can use and share the data in this system. With the
409 increase in the amount of model simulations and observations, and the tediousness of
410 processing data, the shareable approach would be a good way to improve the efficiency
411 of model evaluation. Meanwhile, it can help researchers who develop models focus



412 more on the scientific issues rather than the technical problems.

413 **4.2 Future work**

414 Although TraceME (v1.0) provides a complete and comprehensive system for model
415 evaluation, there are still several aspects must be developed and this work is ongoing.
416 The first one is the traceability analysis method used in TraceME (v1.0). In our current
417 version of TraceME, NPP is finally decomposed into GPP and CUE. However, Xia et
418 al. (2015) has shown GPP is joint controlled by plant phenology and physiology, and it
419 can be decomposed into the carbon dioxide uptake period (CUP; number of days per
420 year) and the maximal daily rate of gross photosynthesis during the CUP (GPP_{max}) that
421 represents a property of plant canopy physiology. GPP_{max} is a critical indicator to
422 quantify the capacity of terrestrial ecosystem productivity (Huang et al., 2018). CUP is
423 related to phenology, which is mainly influenced by environmental factors, such as
424 temperature and water availability (Jaworski and Hilszczański, 2013; Xie et al., 2015;
425 Piao et al., 2019). In addition, Cui et al. (2019) indicates that GPP can be further
426 explained by the subsequent carbon cycle processes and related vegetation functional
427 properties, such as leaf area index and leaf-level photosynthesis. Other environmental
428 factors also affect carbon residence time and NPP, such as atmospheric CO_2 , land-use
429 change, and nitrogen availability (Tian et al., 1999; Wu et al., 2003; Melillo et al., 2011;
430 Van Groenigen et al., 2014; Wieder et al., 2015). These traceable processes can be
431 further added to the traceability analysis framework and applied to TraceME.

432 Secondly, the current version of TraceME focuses on the comparative analysis
433 among multiple models and does not use observation data as benchmarks to analyze
434 model uncertainty. Since the traceability analysis is a systematic analysis method, it
435 requires the time-series observations of all variables used in this system to form a
436 complete benchmarking dataset, such as NPP, GPP and/or net ecosystem exchange
437 (NEE). Some model evaluation systems (e.g. ILAMB and ESMValTool) have built
438 large datasets of observation data (Eyring et al., 2016b; Collier et al., 2018). Particularly,
439 in TraceME, residence time is an important variable for the traceability analysis, and
440 more efforts are still needed to construct a global database of measured C residence
441 time. Wang et al. (2019) have constructed a global soil C residence time database, and
442 used it to evaluate the simulated mean soil C transit times by ESMs. More works are
443 needed to develop the database for TraceME. On the other hand, observed data may



444 have different spatial scales ranging from globe to site, so the future version of TraceME
445 should adapt model evaluation at different scales. Some recent studies have applied the
446 traceability method to analyze the land C storage dynamic at different scales. For
447 example, Jiang et al. (2017) has applied the transient traceability analysis method to
448 compare the difference in ecosystem C dynamics between Duke forest and Harvard
449 forest. Cui et al. (2019) has analyzed the performances of MsTMIP models in
450 simulating ecosystem productivity in the East Asian monsoon region. These analyses
451 could be efficiently applied with the TraceME if the datasets are implemented in the
452 future versions.

453 Lastly, the cyberinfrastructure of TraceME (v1.0) is derived from CAFE. CAFE is
454 a multi-node collaborative platform that can increase the efficiency of performing batch
455 analyses and comparing data from multi-node (Xu et al., 2019). To install CAFE
456 software package in more data centers is an important goal of the development of
457 CAFE, and it involved many computer techniques. For example, Java, Tomcat and
458 MySQL running in a Linux environment are necessary for a CAFE node, and some
459 tools, such as NetCDF Operators (NCO) and Climate Data Operators (CDO), are
460 expected to fulfill data analysis (Xu et al., 2019). Moreover, to better accommodate
461 more data centers, some aspects of CAFE also need further improvement and
462 development. For example, the community tools for publishing new analysis functions,
463 version-control mechanism, intermediate analysis result, and encryption techniques
464 (Xu et al., 2019). The infrastructure of TraceME inherits from CAFE and it is expected
465 to evolve into a more open community for users and developers. These problems in
466 CAFE also need to be addressed in TraceME. Developing more worker nodes is also
467 the inherent requirements for the shareable trait of TraceME, and we also need to
468 develop the infrastructure of TraceME to adapt more data centers. For example, CAFE
469 cannot directly process data from multiple databases on different nodes in a single task
470 because it does not currently have this requirement (Xu et al., 2019). However, in the
471 system of TraceME, there is a need to compare models across data sources, such as
472 models between TRENDY and CMIP. We are working to develop TraceME to support
473 for accessing multiple databases from different nodes in one task. One possible solution
474 is to develop standard interfaces for the results of traceability analysis method on each
475 node, and then aggregate them into one node for the final comparative analysis to
476 reduce data transfers between different nodes. Moreover, the databases in TraceME



(v1.0) need to be updated in a timely and automated manner, especially the amount of benchmarking data products is increasing rapidly (Hoffman et al., 2016). Updating databases more convenient is also a requirement for TraceME's automated computing. Overall, we hope that TraceME can provide a new tool to evaluate global land models and drives the model evaluations on terrestrial biogeochemistry towards traceable in the near future.

Code availability

The code for the traceability analysis is uploaded on <https://doi.org/10.5281/zenodo.3766626>.

Author contributions

JX and JZ designed this study. JZ build the system of TraceME (v1.0). NW provided the support of some algorithms in the system. YB and YF provided the code and technical support of CAFE. JZ wrote the first draft, and all other authors contributed to revision and discussion of the results.

Competing interests

The authors declare that they have no conflict of interest.

Acknowledgements

This work was financially supported by the National Key R&D Program of China (2017YFA0604600) and National Natural Science Foundation of China (31722009). We acknowledge the World Climate Research Program (WCRP) that is responsible for CMIP, and we thank the modelling groups for providing their model output.

References

- Abramowitz, G.: Towards a public, standardized, diagnostic benchmarking system for land surface models, *Geosci. Model. Dev.*, 5, 819-827, 2012.
- Ahlström, A., Schurgers, G., Arneth, A., Smith, B.: Robustness and uncertainty in terrestrial ecosystem carbon response to CMIP5 climate change projections, *Environ. Res. Lett.*, 7, 044008, 2012.



- Bai, Y., Di, L.: Review of geospatial data systems' support of global change studies, *International Journal of Environment and Climate Change*, 2 (4), 421-436, 2012.
- Bonan, G.B., Doney, S.C.: Climate, ecosystems, and planetary futures: The challenge to predict life in Earth system models. *Science* 359, 2018.
- Bonan, G.B., Lombardozzi, D.L., Wieder, W.R., Oleson, K.W., Lawrence, D.M., Hoffman, F.M., Collier, N.J.G.B.C.: Model structure and climate data uncertainty in historical simulations of the terrestrial carbon cycle (1850–2014), *Global. Biogeochem. Cy.*, 33, 2019.
- Chevan, A., Sutherland, M.: Hierarchical Partitioning, *The American Statistician*, 45, 90-96, 1991.
- Collier, N., Hoffman, F.M., Mu, M., Randerson, J.T., Riley, W.J.: International Land Model Benchmarking (ILAMB) Package v002. 00, BGCF-DATA (Biogeochemistry (BGC) Feedbacks), 2016.
- Collier, N., Hoffman, F.M., Lawrence, D.M., Keppel-Aleks, G., Koven, C.D., Riley, W.J., Mu, M., Randerson, J.T.: The International Land Model Benchmarking (ILAMB) System: Design, Theory, and Implementation, *J. Adv. Model. Earth. Sy.*, 10, 2731-2754, 2018.
- Cui, E., Huang, K., Arain, M.A., Fisher, J.B., Huntzinger, D.N., Ito, A., Luo, Y., Jain, A.K., Mao, J., Michalak, A.M., Niu, S., Parazoo, N.C., Peng, C., Peng, S., Poulter, B., Ricciuto, D.M., Schaefer, K.M., Schwalm, C.R., Shi, X., Tian, H., Wang, W., Wang, J., Wei, Y., Yan, E., Yan, L., Zeng, N., Zhu, Q., Xia, J.: Vegetation Functional Properties Determine Uncertainty of Simulated Ecosystem Productivity: A Traceability Analysis in the East Asian Monsoon Region, *Global. Biogeochem. Cy.*, 33, 668-689, 2019.
- DeLucia, E.H., Drake, J.E., Thomas, R.B., Gonzalez-Meler, M.: Forest carbon use efficiency: is respiration a constant fraction of gross primary production? *Global. Change. Biol.*, 13, 1157-1167, 2007.
- Du, Z., Weng, E., Jiang, L., Luo, Y., Xia, J., Zhou, X.: Carbon–nitrogen coupling under three schemes of model representation: a traceability analysis, *Geosci Model Dev*, 11, 4399-4416, 2018.
- Eyring, V., Gleckler, P.J., Heinze, C., Stouffer, R.J., Taylor, K.E., Balaji, V., Guilyardi, E., Joussaume, S., Kindermann, S., Lawrence, B.N., Meehl, G.A., Righi, M., Williams, D.N.: Towards improved and more routine Earth system model evaluation in CMIP, *Earth. Syst. Dynam.*, 7, 813-830, 2016a.
- Eyring, V., Righi, M., Lauer, A., Evaldsson, M., Wenzel, S., Jones, C., Anav, A., Andrews, O., Cionni, I., Davin, E.L., Deser, C., Ehbrecht, C., Friedlingstein, P., Gleckler, P., Gottschaldt, K.-D., Hagemann, S., Juckes, M., Kindermann, S., Krasting, J., Kunert, D., Levine, R., Loew, A., Mäkelä, J., Martin, G., Mason, E., Phillips, A.S., Read, S., Rio, C., Roehrig, R., Senftleben, D., Sterl, A., van Ulft, L.H., Walton, J., Wang, S., Williams, K.D.: ESMValTool (v1.0) – a community diagnostic and performance metrics tool for routine evaluation of Earth system models in CMIP, *Geosci. Model. Dev.*, 9, 1747-1802, 2016b.
- Eyring, V., Cox, P.M., Flato, G.M., Gleckler, P.J., Abramowitz, G., Caldwell, P., Collins, W.D., Gier, B.K., Hall, A.D., Hoffman, F.M., Hurtt, G.C., Jahn, A., Jones, C.D., Klein, S.A., Krasting, J.P., Kwiatkowski, L., Lorenz, R., Maloney, E., Meehl, G.A., Pendergrass, A.G., Pincus, R., Ruane, A.C., Russell, J.L., Sanderson, B.M., Santer, B.D., Sherwood, S.C., Simpson, I.R., Stouffer, R.J., Williamson, M.S.: Taking climate model evaluation to the next level, *Nat. Clim. Change.*, 9, 102-110, 2019a.
- Eyring, V., Bock, L., Lauer, A., Righi, M., Schlund, M., Andela, B., Arnone, E., Bellprat, O., Brötz, B., Caron, L.-P.: ESMValTool v2. 0–Extended set of large-scale diagnostics for quasi-operational and comprehensive evaluation of Earth system models in CMIP, *Geosci. Model. Dev.*, 2019b (in



- discussion).
- Getz, W.M., Marshall, C.R., Carlson, C.J., Giuggioli, L., Ryan, S.J., Romanach, S.S., Boettiger, C., Chamberlain, S.D., Larsen, L., D'Odorico, P., O'Sullivan, D.: Making ecological models adequate. *Ecol. Lett.*, 21, 153-166, 2018.
- Hoffman, F.M., Koven, C.D., Keppel-Aleks, G., Lawrence, D.M., Riley, W.J., Randerson, J.T., Ahlstrom, A., Abramowitz, G., Baldocchi, D.D., Best, M.J.: 2016 International Land Model Benchmarking (ILAMB) Workshop Report, 2016.
- Huang, K., Xia, J., Wang, Y., Ahlstrom, A., Chen, J., Cook, R.B., Cui, E., Fang, Y., Fisher, J.B., Huntzinger, D.N., Li, Z., Michalak, A.M., Qiao, Y., Schaefer, K., Schwalm, C., Wang, J., Wei, Y., Xu, X., Yan, L., Bian, C., Luo, Y.: Enhanced peak growth of global vegetation and its key mechanisms, *Nature Ecology & Evolution*, 2, 1897-1905, 2018.
- Huang, Y., Stacy, M., Jiang, J., Sundi, N., Ma, S., Saruta, V., Jung, C.G., Shi, Z., Xia, J., Hanson, P.J., Ricciuto, D., Luo, Y.: Realized ecological forecast through an interactive Ecological Platform for Assimilating Data (EcoPAD, v1.0) into models, *Geosci. Model. Dev.*, 12, 1119-1137, 2019.
- Jaworski, T., Hilszczański, J.: The effect of temperature and humidity changes on insects development their impact on forest ecosystems in the expected climate change, *Forest Research Papers*, 74, 345-355, 2013.
- Jiang, L., Shi, Z., Xia, J., Liang, J., Lu, X., Wang, Y., Luo, Y.: Transient traceability analysis of land carbon storage dynamics: procedures and its application to two forest ecosystems, *J. Adv. Model. Earth. Sy.*, 9, 2822-2835, 2017.
- Kumar, S.V., Peters-Lidard, C.D., Santanello, J., Harrison, K., Liu, Y., Shaw, M.: Land surface Verification Toolkit (LVT) – a generalized framework for land surface model evaluation, *Geosci. Model. Dev.*, 5, 869-886, 2012.
- LeBauer, D.S., Wang, D., Richter, K.T., Davidson, C.C. and Dietze, M.C.: Facilitating feedbacks between field measurements and ecosystem models, *Ecological Monographs*, 83(2): 133-154, 2013.
- Li, S., Dragicevic, S., Castro, F.A., Sester, M., Winter, S., Coltekin, A., Pettit, C., Jiang, B., Haworth, J., Stein, A.: Geospatial big data handling theory and methods: A review and research challenges, *ISPRS journal of Photogrammetry and Remote Sensing*, 115: 119-133, 2016.
- Lovenduski, N.S., McKinley, G.A., Fay, A.R., Lindsay, K., Long, M.C.: Partitioning uncertainty in ocean carbon uptake projections: Internal variability, emission scenario, and model structure, *Global. Biogeochem. Cy.*, 30, 1276-1287, 2016.
- Luo, Y., Ogle, K., Tucker, C., Fei, S., Gao, C., LaDeau, S., Clark, J.S., Schimel, D.S.J.E.A.: Ecological forecasting and data assimilation in a data-rich era, *Ecol. Appl.*, 21: 1429-1442, 2011.
- Luo, Y., Weng, E.: Dynamic disequilibrium of the terrestrial carbon cycle under global change, *Trends. Ecol. Evol.*, 26, 96-104, 2011.
- Luo, Y., Shi, Z., Lu, X., Xia, J., Liang, J., Jiang, J., Wang, Y., Smith, M.J., Jiang, L., Ahlström, A., Chen, B., Hararuk, O., Hastings, A., Hoffman, F., Medlyn, B., Niu, S., Rasmussen, M., Todd-Brown, K., Wang, Y.-P.: Transient dynamics of terrestrial carbon storage: mathematical foundation and its applications, *Biogeosciences*, 14, 145-161, 2017.
- Luo, Y., Schuur, E.A.: Model parameterization to represent processes at unresolved scales and changing properties of evolving systems, *Global. Change. Biol.*, 26, 1109-1117, 2020.
- Melillo, J.M., Butler, S., Johnson, J., Mohan, J., Steudler, P., Lux, H., Burrows, E., Bowles, F., Smith, R., Scott, L.J.P.o.t.N.A.o.S.: Soil warming, carbon–nitrogen interactions, and forest carbon budgets, *P. Natl. Acad. Sci. USA.*, 108, 9508-9512, 2011.



- 592 Murray, K. & Conner, M. M.: Methods to quantify variable importance: implications for the analysis of
 593 noisy ecological data, *Ecology*, 90, 348-355, 2009.
- 594 Overpeck, J.T., Meehl, G.A., Bony, S., Easterling, D.R.: Climate data challenges in the 21st century,
 595 *Science*, 331, 700-702, 2011.
- 596 Piao, S., Liu, Q., Chen, A., Janssens, I.A., Fu, Y., Dai, J., Liu, L., Lian, X., Shen, M., Zhu, X.: Plant
 597 phenology and global climate change: Current progresses and challenges, *Global. Change. Biol.*, 25,
 598 1922-1940, 2019.
- 599 Rafique, R., Xia, J., Hararuk, O., Asrar, G.R., Leng, G., Wang, Y., Luo, Y.: Divergent predictions of
 600 carbon storage between two global land models: attribution of the causes through traceability
 601 analysis, *Earth. Syst. Dynam.*, 7, 649-658, 2016.
- 602 Rafique, R., Xia, J., Hararuk, O., Leng, G., Asrar, G., Luo, Y.: Comparing the performance of three land
 603 models in global C cycle simulations: a detailed structural analysis, *Land. Degrad. Dev.*, 28, 524-
 604 533, 2017.
- 605 Schwalm, C.R., Williams, C.A., Schaefer, K., Anderson, R., Arain, M.A., Baker, I., Barr, A., Black, T.A.,
 606 Chen, G., Chen, J.M., Ciais, P., Davis, K.J., Desai, A., Dietze, M., Dragoni, D., Fischer, M.L.,
 607 Flanagan, L.B., Grant, R., Gu, L., Hollinger, D., Izaurrealde, R.C., Kucharik, C., Lafleur, P., Law,
 608 B.E., Li, L., Li, Z., Liu, S., Lokupitiya, E., Luo, Y., Ma, S., Margolis, H., Matamala, R., McCaughey,
 609 H., Monson, R.K., Oechel, W.C., Peng, C., Poulter, B., Price, D.T., Riciutto, D.M., Riley, W., Sahoo,
 610 A.K., Sprintsin, M., Sun, J., Tian, H., Tonitto, C., Verbeeck, H., Verma, S.B.: A model-data
 611 intercomparison of CO₂ exchange across North America: Results from the North American Carbon
 612 Program site synthesis, *J. Geophys. Res.*, 115, 2010.
- 613 Shi, Z., Crowell, S., Luo, Y., Moore, B.: Model structures amplify uncertainty in predicted soil carbon
 614 responses to climate change, *Nat. comm.*, 9, 1-11, 2018.
- 615 Song, J., Wan, S., Piao, S., Knapp, A.K., Classen, A.T., Vicca, S., Ciais, P., Hovenden, M.J., Leuzinger,
 616 S., Beier, C., Kardol, P., Xia, J., Liu, Q., Ru, J., Zhou, Z., Luo, Y., Guo, D., Adam Langley, J.,
 617 Zscheischler, J., Dukes, J.S., Tang, J., Chen, J., Hofmockel, K.S., Kueppers, L.M., Rustad, L., Liu,
 618 L., Smith, M.D., Templer, P.H., Quinn Thomas, R., Norby, R.J., Phillips, R.P., Niu, S., Fatichi, S.,
 619 Wang, Y., Shao, P., Han, H., Wang, D., Lei, L., Wang, J., Li, X., Zhang, Q., Li, X., Su, F., Liu, B.,
 620 Yang, F., Ma, G., Li, G., Liu, Y., Liu, Y., Yang, Z., Zhang, K., Miao, Y., Hu, M., Yan, C., Zhang, A.,
 621 Zhong, M., Hui, Y., Li, Y., Zheng, M.: A meta-analysis of 1,119 manipulative experiments on
 622 terrestrial carbon-cycling responses to global change, *Nat. Ecol. Evol.*, 3, 1309-1320, 2019.
- 623 Tian, H., Melillo, J., Kicklighter, D., McGuire, A., Helfrich, J.: The sensitivity of terrestrial carbon
 624 storage to historical climate variability and atmospheric CO₂ in the United States. *Tellus B.*, 51, 414-
 625 452, 1999.
- 626 Todd-Brown, K.E.O., Randerson, J.T., Post, W.M., Hoffman, F.M., Tarnocai, C., Schuur, E.A.G., Allison,
 627 S.D.: Causes of variation in soil carbon simulations from CMIP5 Earth system models and
 628 comparison with observations, *Biogeosciences*, 10, 1717-1736, 2013.
- 629 Van Groenigen, K.J., Qi, X., Osenberg, C.W., Luo, Y., Hungate, B.A.: Faster decomposition under
 630 increased atmospheric CO₂ limits soil carbon storage, *Science*, 344, 508-509, 2014.
- 631 Wang, J., Xia, J., Zhou, X., Huang, K., Zhou, J., Huang, Y., Jiang, L., Xu, X., Liang, J., Wang, Y.-P.,
 632 Cheng, X., Luo, Y.: Evaluating the simulated mean soil carbon transit times by Earth system models
 633 using observations, *Biogeosciences*, 16, 917-926, 2019.
- 634 Wieder, W.R., Cleveland, C.C., Smith, W.K., Todd-Brown, K.J.N.G.: Future productivity and carbon
 635 storage limited by terrestrial nutrient availability, *Nat. Geosci.*, 8, 441-444, 2015.



- 636 Wu, H., Guo, Z., Peng, C.: Land use induced changes of organic carbon storage in soils of China, Global.
 637 Change. Biol., 9, 305-315, 2003.
- 638 Xia, J.Y., Luo, Y.Q., Wang, Y.P., Weng, E.S., Hararuk, O.: A semi-analytical solution to accelerate spin-
 639 up of a coupled carbon and nitrogen land model to steady state, Geosci. Model. Dev., 5, 1259-1271,
 640 2012.
- 641 Xia, J., Luo, Y., Wang, Y.P., Hararuk, O.: Traceable components of terrestrial carbon storage capacity in
 642 biogeochemical models, Global. Change. Biol., 19, 2104-2116, 2013.
- 643 Xia, J., Niu, S., Ciais, P., Janssens, I.A., Chen, J., Ammann, C., Arain, A., Blanken, P.D., Cescatti, A.,
 644 Bonal, D., Buchmann, N., Curtis, P.S., Chen, S., Dong, J., Flanagan, L.B., Frankenberg, C.,
 645 Georgiadis, T., Gough, C.M., Hui, D., Kiely, G., Li, J., Lund, M., Magliulo, V., Marcolla, B.,
 646 Merbold, L., Montagnani, L., Moors, E.J., Olesen, J.E., Piao, S., Raschi, A., Rouspard, O., Suyker,
 647 A.E., Urbaniak, M., Vaccari, F.P., Varlagin, A., Vesala, T., Wilkinson, M., Weng, E., Wohlfahrt, G.,
 648 Yan, L., Luo, Y.: Joint control of terrestrial gross primary productivity by plant phenology and
 649 physiology, P. Natl. Acad. Sci. USA., 112, 2788-2793, 2015.
- 650 Xia, J., McGuire, A.D., Lawrence, D., Burke, E., Chen, G., Chen, X., Delire, C., Koven, C., MacDougall,
 651 A., Peng, S., Rinke, A., Saito, K., Zhang, W., Alkama, R., Bohn, T.J., Ciais, P., Decharme, B.,
 652 Gouttevin, I., Hajima, T., Hayes, D.J., Huang, K., Ji, D., Krinner, G., Lettenmaier, D.P., Miller, P.A.,
 653 Moore, J.C., Smith, B., Sueyoshi, T., Shi, Z., Yan, L., Liang, J., Jiang, L., Zhang, Q., Luo, Y.:
 654 Terrestrial ecosystem model performance in simulating productivity and its vulnerability to climate
 655 change in the northern permafrost region, J. Geophys. Res-Bioge., 122, 430-446, 2017.
- 656 Xie, Y., Wang, X., Silander, J.A., Jr.: Deciduous forest responses to temperature, precipitation, and
 657 drought imply complex climate change impacts, P. Natl. Acad. Sci. USA., 112, 13585-13590, 2015.
- 658 Xu, H., Li, S., Bai, Y., Dong, W., Huang, W., Xu, S., Lin, Y., Wang, B., Wu, F., Xin, X.: A collaborative
 659 analysis framework for distributed gridded environmental data, Environ. Model. Softw., 111, 324-
 660 339, 2019.
- 661 Zhou, S., Liang, J., Lu, X., Li, Q., Jiang, L., Zhang, Y., Schwalm, C.R., Fisher, J.B., Tjiputra, J., Sitch,
 662 S., Ahlström, A., Huntzinger, D.N., Huang, Y., Wang, G., Luo, Y.: Sources of uncertainty in modeled
 663 land carbon storage within and across three mips: diagnosis with three new techniques, J. Climate.,
 664 31, 2833-2851, 2018.
- 665



666 **Table 1** The list of seven ESMs used in this study from CMIP6.

ESM	Land Model	Variables
BCC-ESM1	BCC-AVIM2	
CanESM5	CLASS-CTEM	GPP, NPP
CESM2	CLM5.0	Total vegetation C pool (cVeg)
IPSL-CM6A-LR	ORCHIDEE	Total litter C pool (cLitter)
MIROC-ES2L	VISIT-e	Total soil C pool (cSoil)
CNRM-ESM2-1	ISBA	Precipitation (pr)
EC-Earth3-Veg	LPJ-GUESS	Temperature (tas)

667

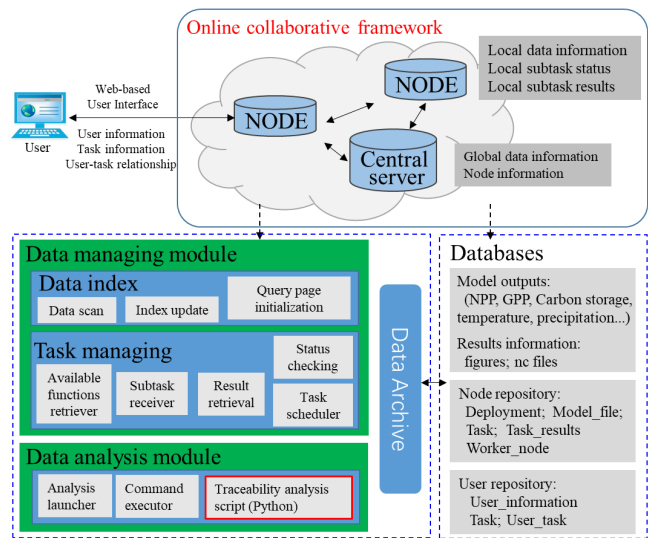
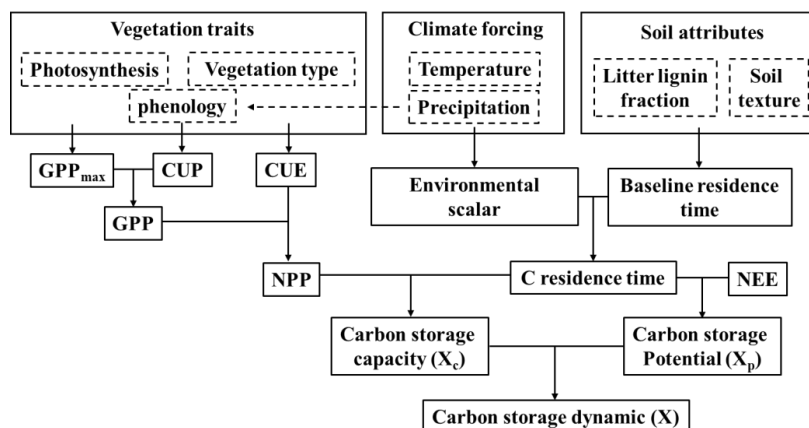
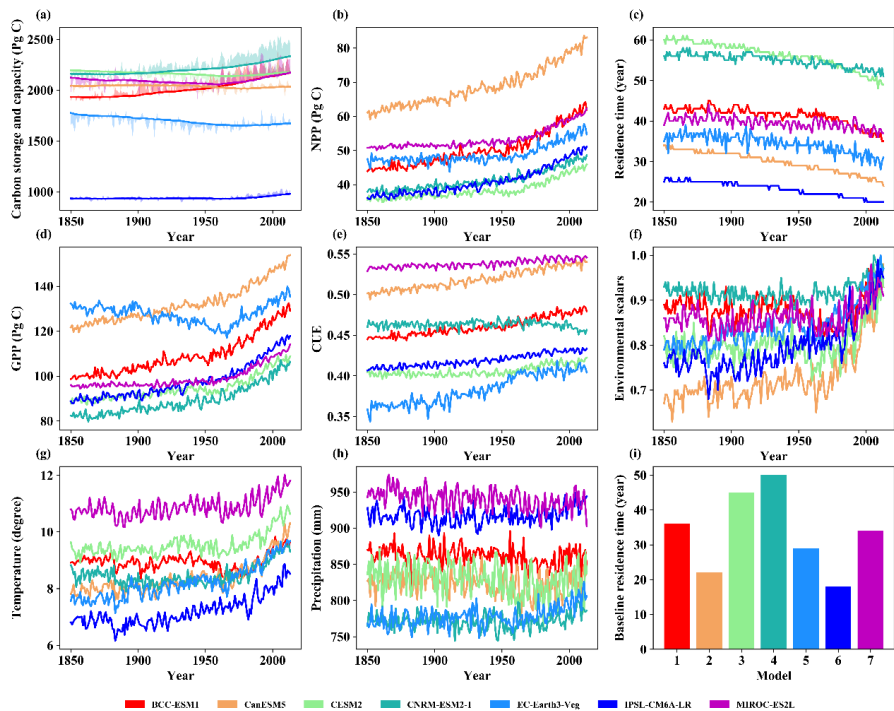


Figure. 1 Schematic overview of TraceME (v1.0).



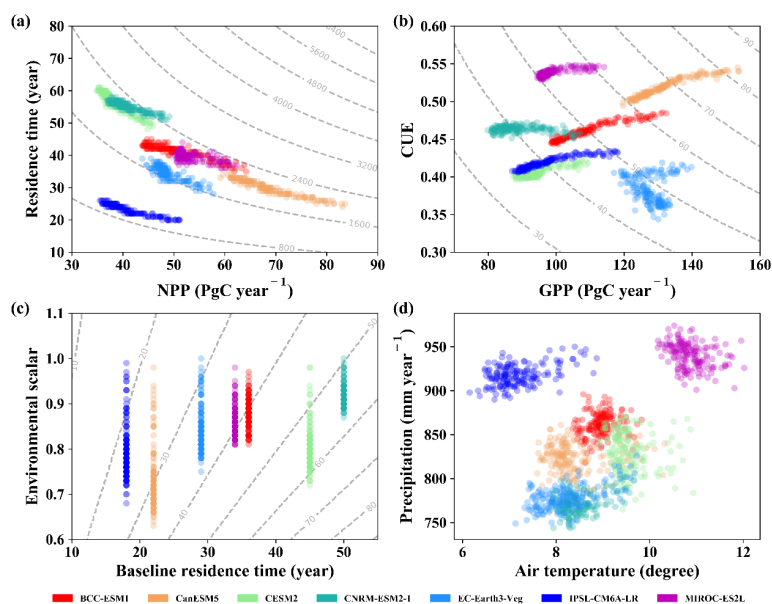
671
 672 Figure. 2 The theoretical framework of traceability analysis. The transient carbon
 673 storage dynamic can be decomposed into carbon storage capacity and potential. Then
 674 the NPP and residence time can explain the carbon storage capacity. NPP can be traced
 675 to GPP and carbon use efficiency (CUE). Residence time can be traced to environmental
 676 scalars and baseline residence time. These traceable components can be explained by
 677 related attributions.
 678



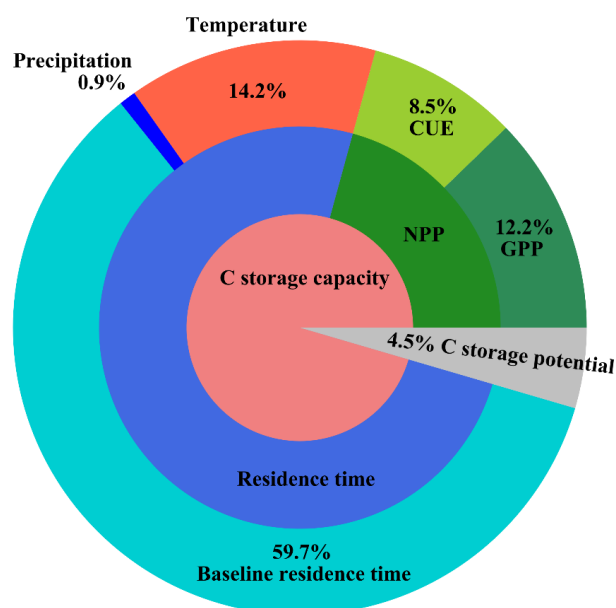
679

680 Figure. 3 The time series of annual carbon storage (solid lines) and carbon storage
681 capacity (the contour lines) (a), and the traceable components: (b)-(h) for NPP,
682 residence time, GPP, CUE, environmental scalars, temperature and precipitation
683 simulated by 7 CMIP6 models, respectively. (i) is the baseline residence time for each
684 model. The shades in (a) represent the annual variation in carbon storage potential for
685 models (positive above the soil lines, and negative below the solid lines).

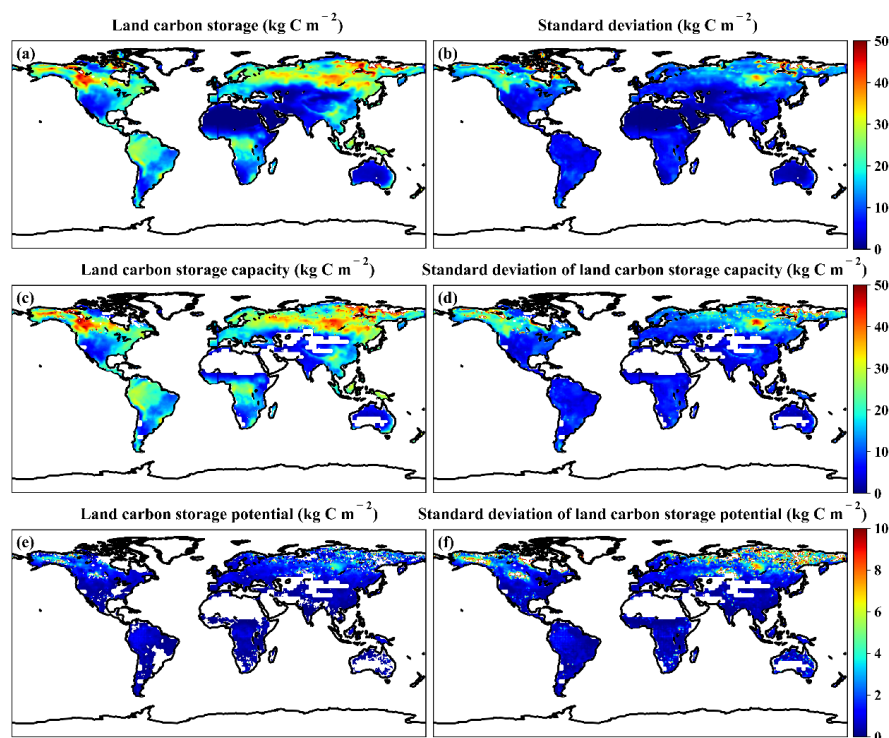
686



687
 688 Figure. 4 The traceability decomposition of carbon storage capacity. The contours lines
 689 in (a)-(c) represent carbon storage capacity, NPP and residence time respectively. Points
 690 represent the global annual values for variables.
 691



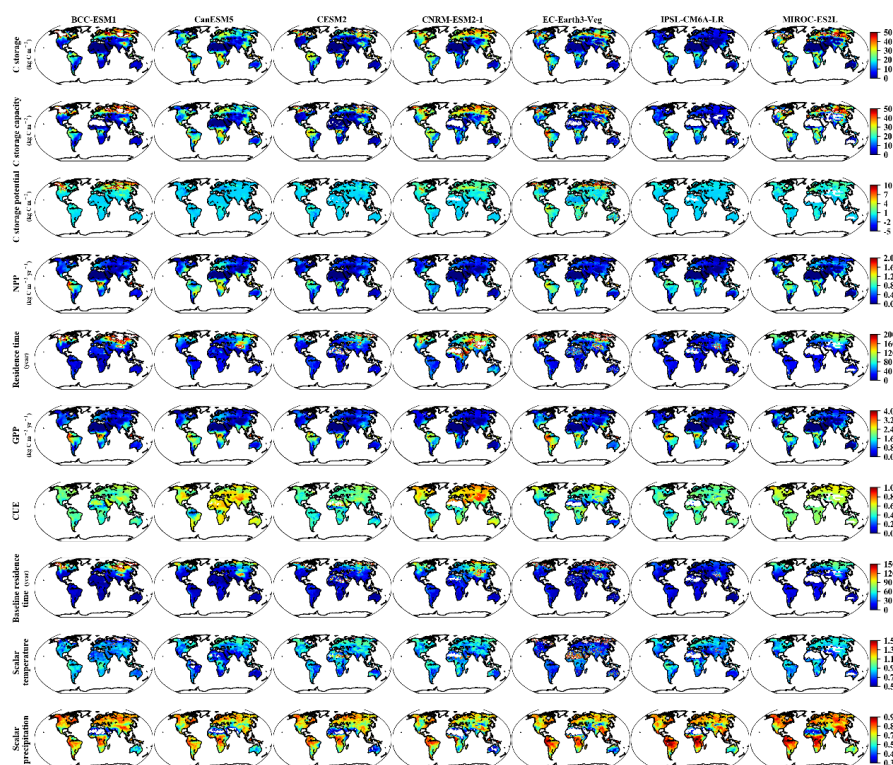
692
 693 Figure. 5 Variation decomposition of the carbon storage based on annual data from
 694 models (CMIP6). The inner circle indicates the carbon storage is composed into carbon
 695 storage capacity and carbon storage potential, and their variance contributions. The
 696 middle circle represents the carbon storage capacity is decomposed into NPP and
 697 residence time, and their variance contributions. The outside circle indicates that the
 698 NPP is decomposed into GPP and CUE, and residence time is decomposed into baseline
 699 residence time and environmental scalars (temperature and precipitation), and their
 700 variation contributions to carbon storage.
 701



702

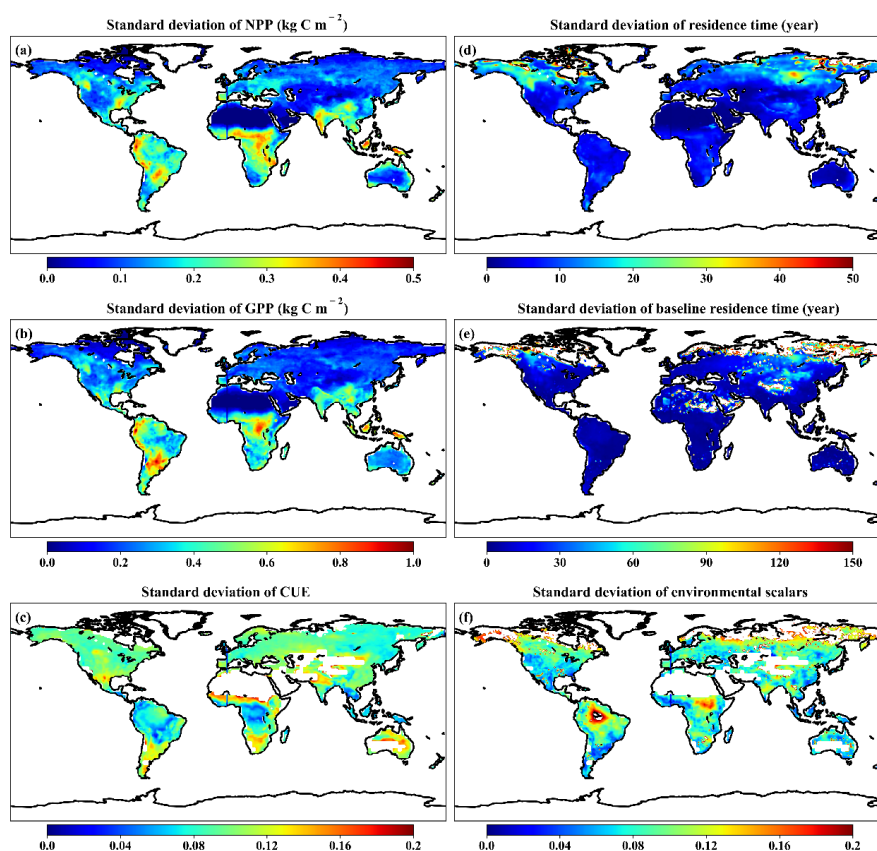
703 Figure. 6 The spatial distribution of the mean land carbon storage (a), land carbon
 704 storage capacity (c) and potential (e) simulated by 7 models from CMIP6 during 1850
 705 to 2014, and the standard deviation of land carbon storage (b), land carbon storage
 706 capacity (d) and potential (f) from these models.

707

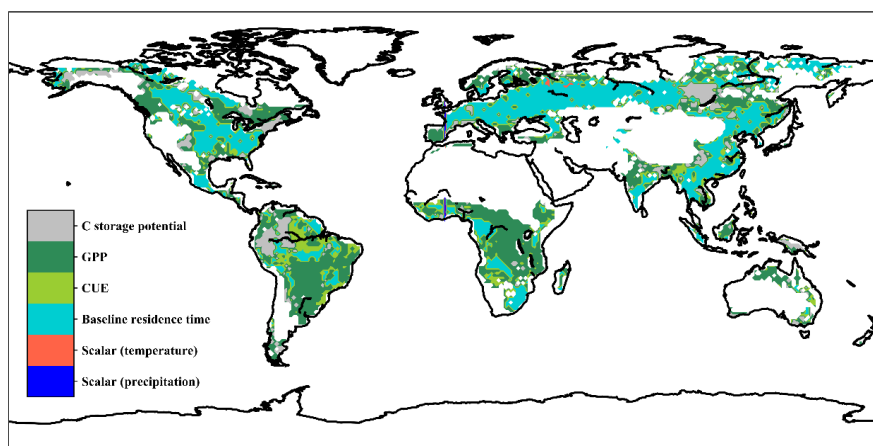


708
 709 Figure. 7 The mean of carbon storage and its traceable components: carbon storage
 710 capacity, carbon storage potential, NPP, residence time, GPP, CUE, baseline residence
 711 time and scalars (temperature and precipitation) simulated by 7 CMIP6 models for the
 712 historical period 1850-2014.

713



714
 715 Figure. 8 The global distribution of the variations of the traceable variables simulated
 716 by 7 models from CMIP6 for the historical period 1850-2014. (a)-(f) represent the
 717 standard deviation of NPP, GPP, CUE, residence time, baseline residence time and
 718 environmental scalars, respectively.
 719



720
 721 Figure. 9 The global distribution of the dominant variable for the variation in simulated
 722 land carbon storage by the models from CMIP6 during 1850 to 2014.

723



727